

PAPER • OPEN ACCESS

## Effect of heat generation on mixed convection of micropolar Casson fluid over a stretching/shrinking sheet with suction

To cite this article: Rahimah Jusoh and Roslinda Nazar 2019 *J. Phys.: Conf. Ser.* **1212** 012024

View the [article online](#) for updates and enhancements.



**IOP | ebooks™**

Bringing you innovative digital publishing with leading voices to create your essential collection of books in STEM research.

Start exploring the collection - download the first chapter of every title for free.

# Effect of heat generation on mixed convection of micropolar Casson fluid over a stretching/shrinking sheet with suction

Rahimah Jusoh<sup>1,2</sup> and Roslinda Nazar<sup>2</sup>

<sup>1</sup> Faculty of Industrial Sciences & Technology, Universiti Malaysia Pahang, 26300 Gambang, Pahang, Malaysia

<sup>2</sup> School of Mathematical Sciences, Faculty of Science and Technology, Universiti Kebangsaan Malaysia, 43600 UKM Bangi, Selangor, Malaysia

E-mail: rahimahj@ump.edu.my

**Abstract.** The problem of mixed convection involving the micropolar Casson fluid over a stretching/shrinking sheet is scrutinized in this study. The sheet is considered permeable with the inclusion of suction. The effect of heat generation is also taken into account. A set of suitable similarity variables is employed to reduce the governing partial differential equations to the ordinary differential equations. The built in `bvp4c` function in Matlab is utilized to solve the resulting ordinary differential equations. Elucidation of numerical results for the skin friction coefficient, Nusselt number and temperature profiles are presented through graphs for a certain range of governing parameters. The existence of non-unique solutions (dual solutions) are also discovered in this study. Final conclusion has been drawn on the effect of variations in suction parameter, Biot number and heat generation parameter and on the flow and heat transfer characteristics. Stability analysis reveals that the first solution is stable while the second solution is unstable.

## 1. Introduction

The rapid growth of manufacturing and processing industries in order to fulfill the higher demands lead to the utilization of new materials which can be categorized as non-Newtonian fluids. One of the material can be modeled as micropolar Casson fluid where micropolar fluid exhibits the behavior of micro-rotational motions, spin inertia and couple stress [1]. Casson fluid is also known as dilatant fluid with infinite viscosity at zero shear rates [2]. As mentioned by Borrelli et al. [3], micropolar fluids have numerous applications in pharmaceutical, chemical, engineering and food industries. Takhar et al. [4] studied mixed convection of micropolar fluid over a stretching sheet and discovered the faster rate of cooling with the larger values of micropolar parameter. Qasim et al. [5] investigated the heat transfer of micropolar fluid and found that the increment of micropolar parameter decreased the thermal boundary layer thickness.

Suction plays an important role in the boundary layer control. Arifin et al. [6] reported that the boundary layer separation can be delayed with the inclusion of suction. Furthermore, the influence of heat generation is also considered in the present study. Eid and Mahny [7] found an enhancement of thermal and concentration boundary layer thickness with a rise in the heat generation parameter. Inspired by the above mentioned studies, the objective of the present work is to investigate the impact of suction and heat generation on the mixed convection of micropolar Casson fluid over a stretching/shrinking sheet. The built in `bvp4c` function in Matlab is applied to generate the numerical results. Since dual



solutions have been discovered, thus stability analysis is conducted to determine the stability characteristic of the solutions.

## 2. Problem formulations

Let us consider the steady two-dimensional flow of an incompressible micropolar Casson fluid over a permeable stretching/shrinking sheet. The sheet is stretched/shrunk in the  $x$ -direction while  $y$ -axis is orthogonal to the surface of the sheet. A uniform ambient temperature  $T_\infty$  is considered and the surface of the sheet is convectively heated at temperature  $T_f$ . The boundary layer equations including the continuity, momentum and energy are given by

$$\frac{\partial u}{\partial x} + \frac{\partial v}{\partial y} = 0, \quad (1)$$

$$u \frac{\partial u}{\partial x} + v \frac{\partial u}{\partial y} = \left( \nu \left( 1 + \frac{1}{\beta} \right) + \frac{\kappa}{\rho} \right) \frac{\partial^2 u}{\partial y^2} + gm(T - T_\infty) + \frac{\kappa}{\rho} \frac{\partial N}{\partial y}, \quad (2)$$

$$u \frac{\partial N}{\partial x} + v \frac{\partial N}{\partial y} = \frac{\Upsilon}{\rho j} \frac{\partial^2 N}{\partial y^2} - \frac{\kappa}{\rho j} \left( 2N + \frac{\partial u}{\partial y} \right), \quad (3)$$

$$u \frac{\partial T}{\partial x} + v \frac{\partial T}{\partial y} = \alpha \frac{\partial^2 T}{\partial y^2} + \frac{Q_0}{\rho C_p} (T - T_\infty), \quad (4)$$

From the above equations,  $u$  and  $v$  are the velocity components in the  $x$ - and  $y$ - directions, respectively,  $\nu$  indicates the kinematic viscosity,  $\beta = \mu_B \sqrt{2\pi_c} / p_y$  is representing the Casson fluid parameter,  $\kappa$  denotes the vortex viscosity,  $g$  indicates the acceleration due to gravity,  $m$  is the coefficient of thermal expansion,  $\rho$  denotes the fluid density,  $\Upsilon = (\mu + \kappa/2)j$  represents the spin radiation viscosity,  $j = \nu/a$  denotes the micro-inertia density,  $\alpha$  is the thermal diffusivity,  $C_p$  is the specific heat at the constant pressure  $p$ ,  $Q_0$  represents the heat generation coefficient and  $N$  is the micropolar rotation velocity.

The governing equations (1)-(4) correspond to the following boundary conditions:

$$u = \lambda u_w(x) = \lambda ax, \quad v = v_w, \quad N = -n \frac{\partial u}{\partial y}, \quad -k \frac{\partial T}{\partial y} = h_f (T_f - T) \quad \text{at } y = 0, \quad (5)$$

$$u \rightarrow 0, \quad N \rightarrow 0, \quad T \rightarrow T_\infty \quad \text{as } y \rightarrow \infty.$$

where  $u_w$  is the velocity at the wall,  $v_w$  denotes the mass transfer velocity,  $n$  is the boundary concentration parameter of fluid,  $k$  denotes the thermal conductivity and  $h_f$  is the heat transfer coefficient.

The following similarity transformations are introduced to solve the above system of partial differential equations:

$$u = a x f'(\eta), \quad v = -\sqrt{av} f(\eta), \quad N = a \sqrt{\frac{a}{\nu}} x h(\eta), \quad \theta(\eta) = \frac{T - T_\infty}{T_f - T_\infty}, \quad \eta = \sqrt{\frac{a}{\nu}} y. \quad (6)$$

Now, equation (1) is fulfilled identically and equations (2)-(4) turn into

$$\left( 1 + \frac{1}{\beta} + K \right) f''' + ff'' - (f')^2 + A\theta + Kh' = 0 \quad (7)$$

$$\left( 1 + \frac{K}{2} \right) h'' + fh' - hf' - K(2h + f'') = 0 \quad (8)$$

$$\theta'' + Prf\theta' + PrQ\theta = 0 \quad (9)$$

correspond to the boundary conditions

$$f(0) = s, \quad f'(0) = \lambda, \quad h(0) = -nf''(0), \quad \theta'(0) = -Bi(1 - \theta(0)), \quad (10)$$

$$f'(\eta) \rightarrow 0, \quad h(\eta) \rightarrow 0, \quad \theta(\eta) \rightarrow 0 \quad \text{as } \eta \rightarrow \infty$$

where  $\lambda$  denotes the constant stretching ( $\lambda > 0$ ) or shrinking ( $\lambda < 0$ ) parameter. Besides,  $K$  denotes the micropolar parameter,  $A$  represents the thermal convective parameter,  $Pr$  is the Prandtl number,  $s$  represents the suction parameter,  $Bi$  is the Biot number and  $Q$  denotes the heat generation parameter which are defined as

$$s = -\frac{v_w}{\sqrt{av}}, \quad Pr = \frac{\nu}{\alpha}, \quad K = \frac{\kappa}{\mu}, \quad A = \frac{Gr_x}{Re_x^2}, \quad Q = \frac{Q_0}{a\rho C_p}, \quad Bi = \frac{h_f}{k} \sqrt{\frac{\nu}{a}}, \quad (11)$$

with  $Gr_x = gm(T_f - T_\infty)x^3/\nu^2$  and  $Re_x = u_w x/\nu$  are the Grashof number and Reynolds number, respectively. The physical quantities of practical interest in this study are the local skin friction coefficients  $C_f$  and the local Nusselt number  $Nu_x$  which can be defined as

$$C_f = \frac{\tau_w}{\rho u_w^2}, \quad Nu_x = \frac{xq_w}{k(T_f - T_\infty)} \quad (12)$$

where the wall friction  $\tau_w$  and the wall heat flux  $q_w$  can be expressed as

$$\tau_w = \left[ \left( \mu + \frac{p_y}{\sqrt{2\pi_c}} + k \right) \frac{\partial u}{\partial y} + \kappa N \right]_{y=0}, \quad q_w = -k \left( \frac{\partial T}{\partial y} \right)_{y=0}. \quad (13)$$

Utilizing the similarity transformations (6), we obtain

$$\sqrt{Re_x} C_f = \left( 1 + \frac{1}{\beta} + K(1-n) \right) f''(0), \quad \sqrt{1/Re_x} Nu_x = -\theta'(0). \quad (14)$$

### 3. Stability Analysis

Stability analysis is necessary in this study to identify the reliability of the dual solutions. Merkin [8] reported that the stability analysis can be done by considering the time-dependent problem. Thus, the unsteady case for equations (2)-(4) is considered as follows:

$$\frac{\partial u}{\partial t} + u \frac{\partial u}{\partial x} + v \frac{\partial u}{\partial y} = \left( \nu \left( 1 + \frac{1}{\beta} \right) + \frac{\kappa}{\rho} \right) \frac{\partial^2 u}{\partial y^2} + gm(T - T_\infty) + \frac{\kappa}{\rho} \frac{\partial N}{\partial y}, \quad (15)$$

$$\frac{\partial N}{\partial t} + u \frac{\partial N}{\partial x} + v \frac{\partial N}{\partial y} = \frac{\Upsilon}{\rho j} \frac{\partial^2 N}{\partial y^2} - \frac{\kappa}{\rho j} \left( 2N + \frac{\partial u}{\partial y} \right), \quad (16)$$

$$\frac{\partial T}{\partial t} + u \frac{\partial T}{\partial x} + v \frac{\partial T}{\partial y} = \alpha \frac{\partial^2 T}{\partial y^2} + \frac{Q_0}{\rho C_p} (T - T_\infty), \quad (17)$$

where  $t$  representing the time. As suggested by Weidman et al. [9], a new dimensionless time variable  $\tau$  need to be applied. Thus, the new similarity variables are

$$u = ax \frac{\partial f}{\partial \eta}(\eta, \tau), \quad v = -\sqrt{av} f(\eta, \tau), \quad N = a \sqrt{\frac{a}{\nu}} xh(\eta, \tau), \quad (18)$$

$$\theta(\eta, \tau) = \frac{T - T_\infty}{T_f - T_\infty}, \quad \eta = \sqrt{\frac{a}{\nu}} y, \quad \tau = at.$$

The following equations are obtained by substituting the new variables (18) into equations (2)-(4):

$$\left( 1 + \frac{1}{\beta} + K \right) \frac{\partial^3 f}{\partial \eta^3} + f \frac{\partial^2 f}{\partial \eta^2} - \left( \frac{\partial f}{\partial \eta} \right)^2 + A\theta + K \frac{\partial h}{\partial \eta} - \frac{\partial^2 f}{\partial \eta \partial \tau} = 0, \quad (19)$$

$$\left( 1 + \frac{K}{2} \right) \frac{\partial^2 h}{\partial \eta^2} + f \frac{\partial h}{\partial \eta} - h \frac{\partial f}{\partial \eta} - K \left( 2h + \frac{\partial^2 f}{\partial \eta^2} \right) - \frac{\partial h}{\partial \tau} = 0, \quad (20)$$

$$\frac{\partial^2 \theta}{\partial \eta^2} + Pr \left( f \frac{\partial \theta}{\partial \eta} + Q\theta - \frac{\partial \theta}{\partial \tau} \right) = 0, \quad (21)$$

subject to the boundary conditions

$$f(0, \tau) = s, \quad \frac{\partial f}{\partial \eta}(0, \tau) = \lambda, \quad h(0, \tau) = -n \frac{\partial^2 f}{\partial \eta^2}(0, \tau), \quad \frac{\partial \theta}{\partial \eta}(0, \tau) = -Bi(1 - \theta(0, \tau)),$$

$$\frac{\partial f}{\partial \eta}(\infty, \tau) \rightarrow 0, \quad h(\infty, \tau) \rightarrow 0, \quad \theta(\infty, \tau) \rightarrow 0.$$
(22)

Following [10–12], the stability characteristic of the steady flow solution  $f = f_0(\eta)$ ,  $h = h_0(\eta)$  and  $\theta = \theta_0(\eta)$  can be tested by considering

$$f(\eta, \tau) = f_0(\eta) + e^{-\gamma \tau} F(\eta), \quad h(\eta, \tau) = h_0(\eta) + e^{-\gamma \tau} H(\eta), \quad \theta(\eta, \tau) = \theta_0(\eta) + e^{-\gamma \tau} J(\eta),$$
(23)

where  $\gamma$  is an unknown eigenvalue parameter which determining the linear stability of the flow, and  $F(\eta)$ ,  $H(\eta)$  and  $J(\eta)$  are small relative to  $f_0(\eta)$ ,  $h_0(\eta)$  and  $\theta_0(\eta)$ . Solutions of the equations (19)–(22) yields a sequence of eigenvalues  $\gamma_1 < \gamma_2 < \gamma_3 \dots$  and the stability is determined by the lowest eigenvalue  $\gamma_1$ . Substitution of (23) into (19)–(21) produces the following linearized equations:

$$\left(1 + \frac{1}{\beta} + K\right) F''' + f_0 F'' + F f_0'' - 2f_0' F' + AJ + KH' + \gamma F' = 0$$
(24)

$$\left(1 + \frac{K}{2}\right) H'' + f_0 H' + F h_0' - h_0 F' - H f_0' - K(2H + F'') + \gamma H = 0$$
(25)

$$J'' + Pr \left[ f_0 J' + F \theta_0' + QJ + \gamma J \right] = 0$$
(26)

along with the boundary conditions

$$F(0) = 0, \quad F'(0) = 0, \quad H(0) = -nF''(0), \quad J'(0) = BiJ(0),$$

$$F'(\infty) \rightarrow 0, \quad H(\infty) \rightarrow 0, \quad J(\infty) \rightarrow 0.$$
(27)

As mentioned by Harris et al. [13], relaxation of any boundary condition on  $F'(\eta)$ ,  $H(\eta)$  or  $J(\eta)$  provides the range of possible eigenvalues. In this study, the condition  $F'(\eta) \rightarrow 0$  as  $\eta \rightarrow \infty$  is chosen to be relaxed. Then, a new boundary condition  $F''(0) = 1$  is applied to solve the system of equations (24)–(27).

#### 4. Results and discussion

For validation purposes, the present results have been compared with Qasim et al. [5]. They used Runge-Kutta-Fehlberg fourth-fifth order method to generate the numerical results. As depicted in Table 1, the present results are in excellent agreement with Qasim et al. [5] which verify the numerical method used in this study.

**Table 1.** Comparison of  $(\text{Re}_x)^{1/2} C_f$  for different values of  $K$  and  $n$  when  $s = \beta = Q = 0$  and  $Pr = 3$

$K$	$n = 0$		$n = 0.5$	
	Qasim et al. [5]	Present	Qasim et al. [5]	Present
0	-1.000000	-1.000000	-1.000000	-1.000000
1	-1.367872	-1.367931	-1.224741	-1.224745
2	-1.621225	-1.621339	-1.414218	-1.414214
4	-2.004133	-2.004238	-1.732052	-1.732054
5	–	-2.162770	–	-1.870838

**Table 2.** Smallest eigenvalue,  $\gamma_1$  for some values of  $\lambda$

$\lambda$	$\gamma_1$ (first solution)	$\gamma_1$ (second solution)
-0.5	1.2860	-1.9809
-1	0.7776	-0.8082
-1.1	0.6488	-0.6738
-1.14	0.2623	-0.1352
-1.1407	0.0194	-0.0117

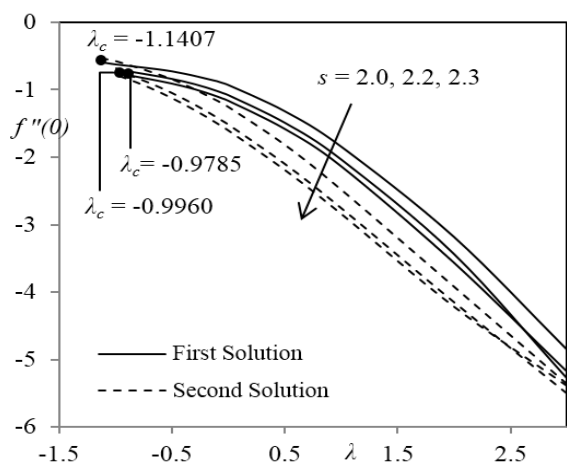


**Figure 1.** Variations of  $f''(0)$  for some values of  $s$  when  $Pr = 0.72$ ,  $A = \beta = Bi = 0.5$ ,  $K = 5$ , and  $Q = 1$ .

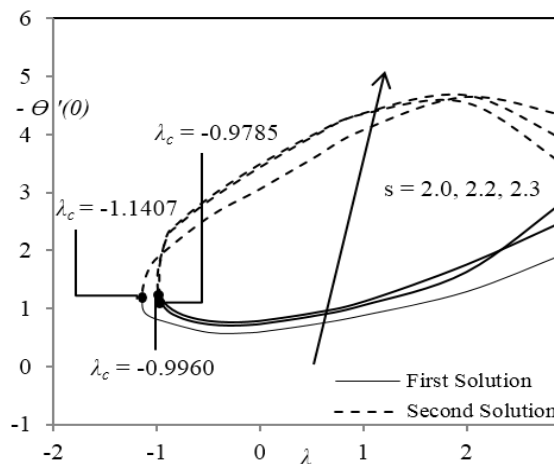


**Figure 2.** Variations of  $-\theta'(0)$  for some values of  $s$  when  $Pr = 0.72$ ,  $A = \beta = Bi = 0.5$ ,  $K = 5$ , and  $Q = 1$ .

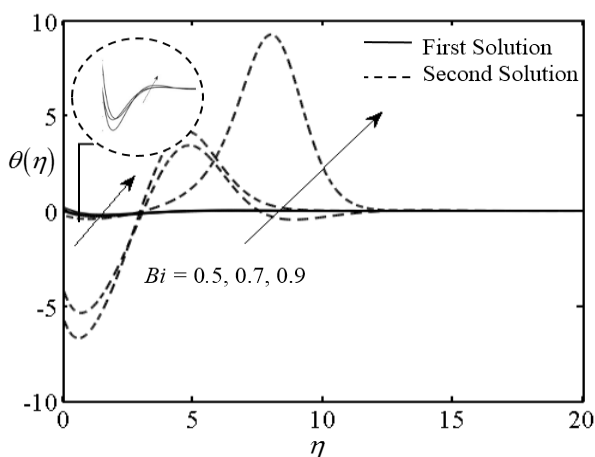


**Figure 3.** Temperature profiles  $\theta(\eta)$  for some values of  $Bi$  when  $K = 5$ ,  $Pr = 0.72$ ,  $\lambda = -0.05$ ,  $A = \beta = 0.5$  and  $Q = 1$ .

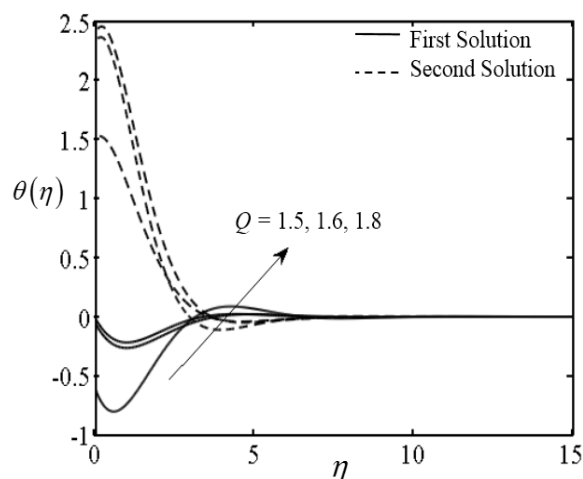


**Figure 4.** Temperature profiles  $\theta(\eta)$  for some values of  $Q$  when  $\lambda = -0.05$ ,  $A = \beta = Bi = 0.5$ ,  $K = 5$  and  $Pr = 0.72$ .

Dual solutions exist for a certain range of governing parameters as shown in Figures 1-4. Stability analysis has been conducted to test the stability behaviour of the solutions by determining the smallest

eigenvalue  $\gamma_1$ . As listed in Table 2, positive values of  $\gamma_1$  are obtained for the first solution which reflecting the stability behavior of the first solution. Conversely, the values of  $\gamma_1$  for the second solution are negative which means that there exist an initial growth of disturbances. Therefore, the second solution is unstable.

Figures 1 and 2 portray the effect of suction to the reduced skin friction coefficient and the local Nusselt number, respectively. An increment in the suction parameter increases the value of  $|f''(0)|$  since suction exerts a dragging force on the fluid. As a result, the rate of heat transfer also increases with the enlargement of  $s$ . Figures 3 and 4 show an upsurge of temperature profiles with the increment of Biot number and heat generation, respectively. Since Biot number is inversely proportional to the thermal resistance, thus the hot fluid side convection resistance is deteriorating as  $Bi$  increases. Therefore, this implies a higher surface temperature. In addition, increasing value of  $Q$  generates more heat in the flow region and consequently rises the temperature of the fluid.

## 5. Conclusions

The effects of suction and heat generation on the mixed convection of micropolar Casson fluid over a stretching/shrinking sheet were investigated. The governing equations of the problem were numerically solved by using the `bvp4c` function in Matlab. Dual solutions were discovered for a certain range of governing parameters. Therefore, stability analysis was conducted to test the stability behavior of both solutions. By referring to the smallest eigenvalue, the first solution is found to be stable whereas the second solution is not stable. The inclusion of suction led to a drag force and increased the skin friction coefficient. This circumstance indirectly enhanced the rate of heat transfer. In addition, the enlargement of the Biot number and heat generation parameter boosted the higher fluid's temperature.

## Acknowledgement

This study was financially supported by the research university grant (No. DIP-2017-009) from the Universiti Kebangsaan Malaysia.

## References

- [1] Eringen A C 1966 *J. Math. Mech.* **16** 1–18
- [2] Mehmood Z, Mehmood R, Iqbal Z 2017 *Commun. Theor. Phys.* **67** 443–448
- [3] Borrelli A, Giancesio G, Patria M C 2015 *Commun. Nonlinear Sci. Numer. Simul.* **20** 121–135
- [4] Takhar H S, Agarwal R S, Bhargava R, Jain S 1998 *Heat Mass Transf.* **34** 213–219
- [5] Qasim M, Khan I, Shafie S 2013 *PLoS ONE* **8** e59393
- [6] Arifin N M, Nazar R, Pop I 2011 *Sains Malaysiana* **40** 1359–1367
- [7] Eid M R, Mahny K L 2017 *Adv. Powder. Technol.* **28** 3063–3073
- [8] Merkin J H 1985 *J. Eng. Math.* **20** 171–179
- [9] Weidman P D, Kubitschek D G, Davis A M J 2006 *Int. J. Eng. Sci.* **44** 730–737.
- [10] Pop I, Naganthran K, Nazar R, Ishak A 2016 *Int. J. Numer. Methods Heat Fluid Flow* **27** 1910–19270
- [11] Weidman P, Turner M R 2017 *Eur. J. Mech. B/Fluids* **61** 144–153
- [12] Jusoh R, Nazar R, Pop I. 2018 *J. Magn. Magn. Mater.* **465** 365–374
- [13] Harris S D, Ingham D B, Pop I 2009 *Transp. Porous Media* **77** 267–285